IIETA International Information and Engineering Technology Association
Advancing the World of Information and Engineering

Journal Européen des Systèmes Automatisés
Vol. 59, No. 9, September, 2026, pp. 2429-2436
Journal homepage: http://iieta.org/journals/jesa

# A Critical and Mechanism-Based Review of Tailor Welded Blanks in Sheet Metal Forming: Formability, Weld Line Movement, and Failure

Hussein Ali Salman[1*], Sara Saad Ghazi[1], Ahmed Abdullah Ebraheem[2], Rawaa Hamid Al Kalali[1]

[1] Polytechnic College for Engineering, Middle Technical University, Baghdad 10074, Iraq
[2] Aeronautical Technical Engineering, College of Engineering Techniques, Al-Farahidi University, Baghdad 10013, Iraq

Corresponding Author Email: hussein_ali33@mtu.edu.iq

Copyright: ©2026 The authors. This article is published by IIETA and is licensed under the CC BY 4.0 license (http://creativecommons.org/licenses/by/4.0/).

https://doi.org/10.18280/jesa.590901

**Received:** 26 May 2026
**Revised:** 2 August 2026
**Accepted:** 13 August 2026
**Available online:** 30 September 2026

***Keywords:***
*tailor-welded blanks, deep drawing, sheet metal formability, weld-line movement, weld-zone heterogeneity, failure mechanisms, automated forming control*

**ABSTRACT**

Tailor-welded blanks (TWBs) combine sheets of different thickness, grade, or surface condition before forming to reduce mass and place strength where it is required. This critical review uses a documented structured-narrative search to examine how material mismatch, weld-zone heterogeneity, boundary conditions, and local strain paths interact during deep drawing, with other forming routes treated separately. The synthesis centers on weld-line movement (WLM), localization, failure, and springback rather than on welding processes in isolation. Formability ratio (FR), strength ratio (SR), and limit strength ratio (LSR) are restored with explicit definitions and applicability limits. Evidence shows that the direction of WLM is not universal: it depends on the coordinate convention, the measured region of the formed part, weld placement, draw-in, and the local resistance field. Material and thickness mismatch remain major drivers, but fusion-zone and heat-affected-zone properties, residual stress, weld width and geometry, anisotropy, friction, and blank-holder control can be equally consequential in specific material-process systems. Failure is therefore classified by both location and trigger, including weld-metal fracture, heat-affected-zone localization, weaker-base-sheet necking, edge or interface initiation, and mixed modes under non-linear strain paths. Friction stir welding (FSW) can reduce melting-related degradation in selected aluminum and dissimilar systems, but its benefits are conditional on tool design, parameter control, local softening, interface defects, surface quality, tool wear, and production rate. The review concludes with a mechanism map and an automation-oriented research agenda involving weld-zone property mapping, online WLM monitoring, finite element (FE)-experiment updating, data-driven quality prediction, and closed-loop control of blank holding and drawbead restraint.

## 1. INTRODUCTION

Tailor-welded blanks (TWBs) join sheets of different thickness, strength, grade, or coating before forming so that mass and load-bearing capacity can be distributed locally. Their industrial value is established, but the joined blank is mechanically heterogeneous: the base sheets, weld metal or stir zone, heat-affected zone (HAZ), and residual-stress field create a spatially varying resistance to plastic flow [1-3].

For deep drawing, the central problem is not simply whether a joint is strong enough. Thickness and strength mismatch alter draw-in; weld placement changes the strain path; local softening or hardening redirects deformation; and blank-holder force (BHF), friction, and tooling determine whether mismatch is accommodated or amplified. These coupled effects govern weld-line movement (WLM), localization, fracture, springback, and dimensional accuracy [2, 4-6].

This review therefore asks three mechanism-based questions: (1) how the material and weld-zone resistance map controls local flow, (2) why WLM direction and failure location change with forming context, and (3) how sensing, finite element (FE) models, and adaptive restraint could improve prediction and automated control. Deep drawing is the primary scope; stretch forming, warm forming, hydraulic bulging, single-point incremental forming, and bending are synthesized separately because their stress states and formability metrics are not interchangeable.

The paper first defines the review method and mechanism framework, then examines formability measures, welding-process effects, failure taxonomy, WLM, and springback. Evidence is grouped by forming process before the implications for online monitoring, data-driven quality prediction, and closed-loop forming control are discussed.

A structured narrative review was conducted for publications dated January 2014 to December 2025. Searches combined Scopus, Web of Science, ScienceDirect, SpringerLink, Taylor & Francis Online, and Google Scholar citation chasing. Search strings combined ‘tailor welded blank’ with ‘deep drawing’, ‘formability’, ‘weld line movement’, ‘failure’, ‘heat-affected zone’, ‘springback’, ‘friction stir welding’, ‘finite element’, ‘monitoring’, ‘machine learning’, and ‘process control’. Older studies were

retained only when they introduced a metric, mechanism, or benchmark repeatedly used by the recent literature.

Included studies were peer-reviewed journal articles that reported a material system and at least one forming, weld-zone, WLM, failure, springback, or control outcome relevant to TWBs. Conference summaries without sufficient methods, generic sheet-forming papers without a welded blank, tailor-rolled or additively tailored blanks without a welded interface, vendor resources, incomplete records, and ResearchGate-only placeholders were excluded. The final evidence base contains 30 verifiable publications: 23 from 2014-2025 and seven foundational earlier papers identified by backward citation.

Evidence was synthesized by forming process rather than pooled. Deep drawing and stamping studies form the principal group; stretch/bulge forming, warm forming, single-point incremental forming, and bending/unloading are treated as separate process groups. The comparison matrix records material system, thickness information when reported, welding method, forming process, principal metric, WLM direction or failure mode, and the main limitation of transfer to other processes. This protocol is structured and reproducible but is not claimed as a PRISMA systematic review or meta-analysis.

## 2. MECHANISM-BASED FRAMEWORK

Figure 1 links the variables that are otherwise discussed separately. Material mismatch and the weld-zone state define a spatial resistance map; process boundary conditions determine how that map is sampled by the evolving local strain path. Their interaction produces location-dependent WLM, localization or fracture, and non-uniform unloading. The framework prevents any single factor—such as strength ratio (SR) or welding method—from being treated as universally dominant.

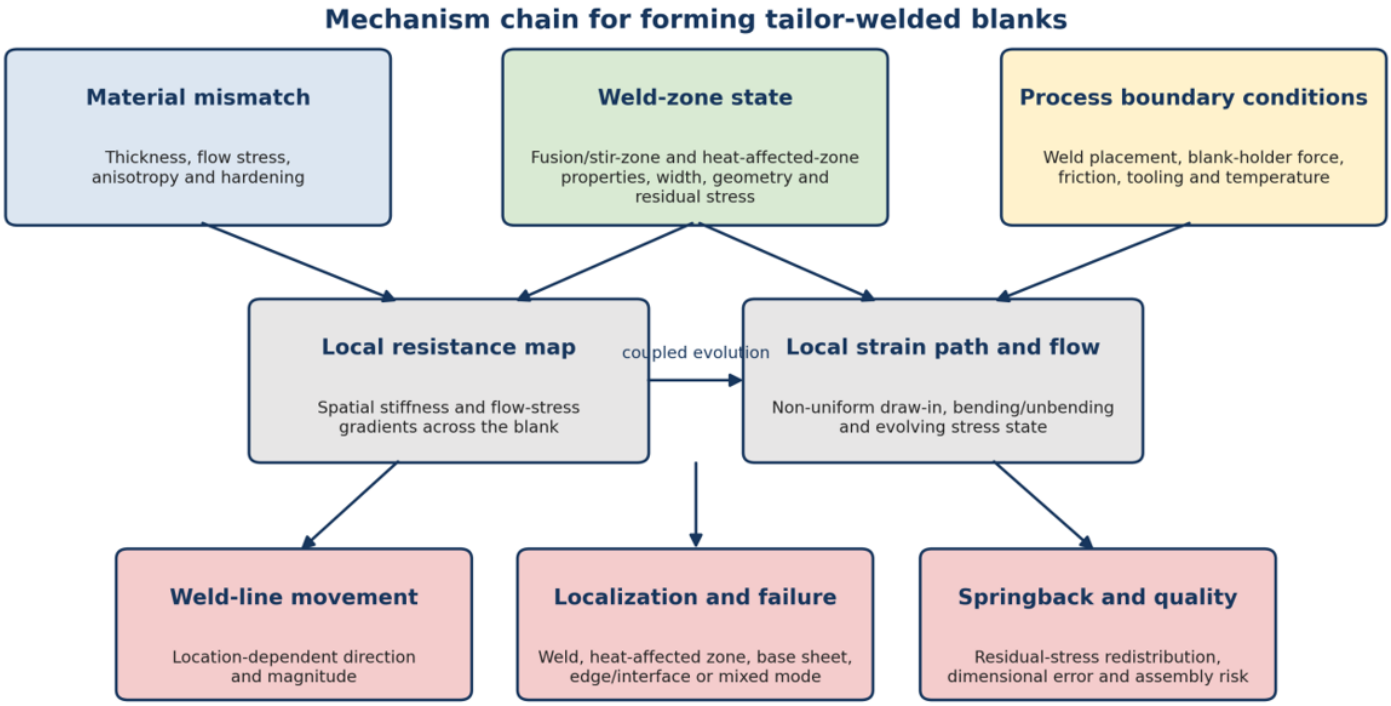



**Figure 1.** Mechanism map for forming a tailor-welded blank (TWB): material mismatch, weld-zone properties, and process boundary conditions jointly govern the local strain path, weld-line movement (WLM), failure, and springback

## 3. TAILOR-WELDED BLANKS: CONCEPT AND DESIGN TRADE-OFFS

TWBs are sheet assemblies produced by joining sheets with different thicknesses, grades, coatings, or mechanical properties before forming. They allow high-strength or thick material to be placed only where load or crash performance requires it, while lighter or more formable sheet is used elsewhere [1, 7].

The same tailoring creates the core forming challenge. A TWB contains at least two base-material responses plus a weld or stir zone and, for thermally affected processes, a HAZ. The joint can therefore alter stiffness, flow stress, hardening, anisotropy, ductility, surface topography, and residual stress across a narrow spatial interval [3, 8, 9].

The design benefit and forming penalty must be evaluated together. A useful TWB design is not merely the lightest material distribution or the strongest joint; it is a blank whose local resistance field, weld placement, tooling, and restraint produce stable flow without unacceptable WLM, thinning, fracture, or springback.

## 4. FORMABILITY MEASURES AND REFERENCE CONDITIONS

Deep-drawing evidence is commonly summarized by the limiting drawing ratio (LDR), defined as the largest successfully drawn blank diameter divided by punch diameter. For comparisons between a TWB and a parent sheet, the formability ratio (FR) normalizes LDR, SR represents the tensile load-capacity mismatch across the weld [4, 10].

For a two-sheet blank with strong side s and weak side w, the simplified definitions are given in Eqs. (1) and (2) [10]. Thickness is included in SR because the relevant section force

scales with strength times sheet thickness. These ratios are comparison indicators, not constitutive laws; they are valid only when the same test geometry, loading protocol, and reference-material convention are used.

$$SR = (\sigma u,s \times ts) / (\sigma u,w \times tw) \quad (1)$$

$$FR = LDRTWB / LDRref \quad (2)$$

Here, σu is ultimate tensile strength, t is initial sheet thickness, s and w denote the stronger and weaker sheet in the loading direction, LDRTWB is the limiting drawing ratio of the welded blank, and LDRref is the LDR of the explicitly identified higher-ductility parent sheet. Figure 2 illustrates the relationship between SR, formability, and WLM in the cited material pair [10].

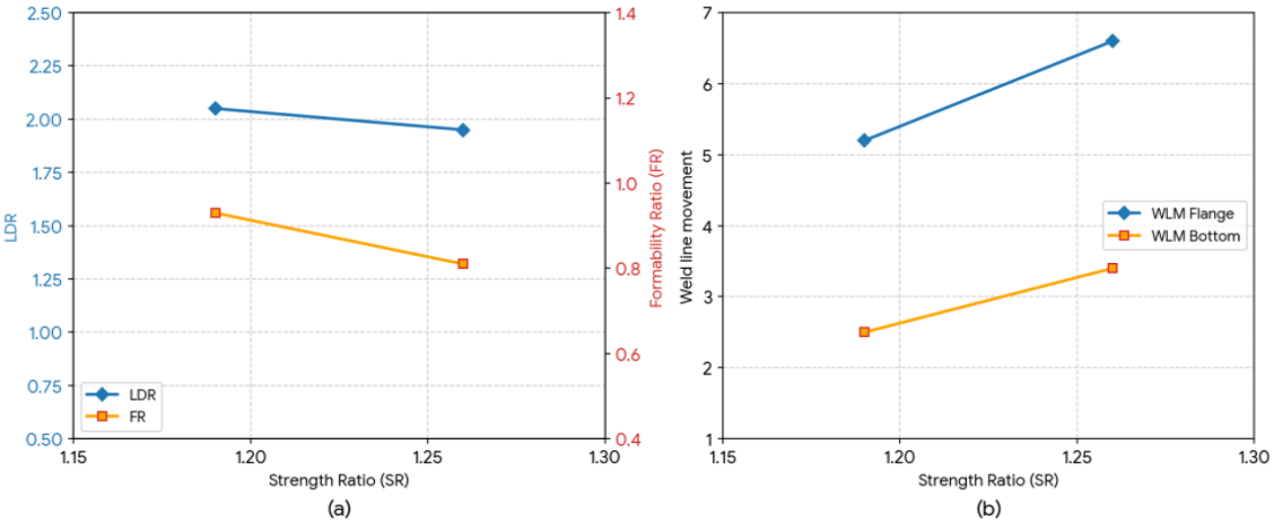



**Figure 2.** Redrawn based on data from Mayavan et al. [10] for 0.8 mm laser-welded AISI 304-IS 513 CR2 and CR3: (a) limiting drawing ratio (LDR) and formability ratio (FR) versus strength ratio (SR); (b) weld-line movement (WLM) magnitude at the flange and cup bottom. Bottom movement was toward AISI 304 and flange movement toward IS 513; SR = 1.194 and 1.263, respectively

Weld orientation changes the local strain path and the projection of material flow across the interface. Orientations that reduce normal strain transfer across a high-mismatch weld can delay localization, but the benefit depends on blank geometry, loading path, anisotropy, and weld-zone properties; orientation is therefore not a universally independent design variable [11, 12].

For equal-thickness sheets under the simplified force-balance assumption used in forming-limit analysis, the limit strength ratio (LSR) compares the first yield of the stronger sheet with the maximum nominal tensile resistance of the weaker sheet [13].

$$LSR = \sigma y,s / \sigma u,w \quad (3)$$

In Eq. (3), σy,s is the yield strength of the stronger sheet and σu,w is the ultimate tensile strength of the weaker sheet. For unequal thickness, the corresponding section-force comparison must include ts/tw; the equal-thickness expression must not be applied without that qualification.

The LSR is a screening criterion tied to the assumed uniaxial material response and strain-path approximation. It does not replace a forming-limit curve, damage model, weld-zone constitutive map, or experiment under the actual loading path [13].

Formability can be improved by redistributing draw-in with segmented binders, tailored tools, adjustable drawbeads, counter pressure, local heat treatment, or an offset weld. Each strategy modifies boundary conditions or the local resistance field and must be optimized for the particular sheet pair and geometry [5, 6, 10, 14-16].

Increasing strength or thickness mismatch often increases strain concentration in the more deformable sheet, but the effect is not monotonic across all processes. Weld-zone softening or hardening, weld width and geometry, residual stress, friction, and location relative to a high-strain region can amplify, suppress, or relocate the instability [8, 9, 11, 17, 18].

Accordingly, LDR, FR, SR, and LSR should be reported with their reference sheet, thicknesses, weld process, weld-zone model, forming path, and failure criterion. Comparisons lacking these conditions can be directionally useful but should not be treated as transferable design limits.

## 5. WELDING PROCESSES AND WELD-ZONE HETEROGENEITY

The joining route defines more than joint strength. It establishes the width, geometry, microstructure, hardness, ductility, residual-stress state, and surface condition of the fusion zone or stir zone and the adjacent HAZ. These fields enter the forming problem directly through the local resistance map [3, 8, 9].

Processes reported for TWBs include laser beam welding (LBW), friction stir welding (FSW), plasma arc welding (PAW), and mash-seam resistance welding (MSRW). Comparisons must be stratified by material system because a process that is advantageous for an aluminum pair may not be practical or defect-tolerant for coated steels or an aluminum-steel interface [19-22].

LBW provides a narrow weld and high production rate, but local hardening in advanced high-strength steels, soft zones adjacent to the fusion zone, porosity, underfill, and residual stress can still govern localization. MSRW has different weld

width and surface geometry and therefore cannot be represented by the same local constitutive strip without calibration.

A mechanically useful model assigns the two base sheets and the weld/HAZ separate, spatially resolved properties rather than treating the weld as a rigid line or omitting it. Simplified models may be adequate when the weld is narrow and stronger than both sheets, but they can be non-conservative when local softening, interface behavior, or weld geometry controls failure [3, 8, 9]. The heterogeneous sheet and weld-zone structure of a TWB is illustrated in Figure 3 [3].

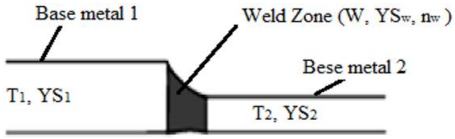



**Figure 3.** Typical structure of a tailor-welded blank (TWB) with dissimilar sheet thicknesses and strengths and a distinct weld-zone property field [3]

FSW is a solid-state option that can limit melting-related defects and produce useful formability in selected aluminum and dissimilar-material TWBs. Its performance, however, is conditional rather than generally superior to fusion welding [19-22].

During FSW, a rotating tool generates frictional heat and severe plastic flow below the bulk melting temperature. Tool geometry, plunge depth, tilt, rotational speed, traverse speed, and material placement control heat input, mixing, interface morphology, surface condition, and the width of locally softened or hardened zones. The heat-generation and material-flow mechanism of FSW is illustrated in Figure 4 [19].

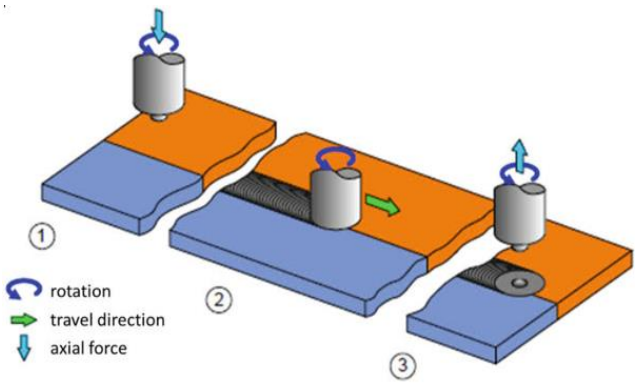



**Figure 4.** Schematic mechanism of friction stir welding (FSW), in which a rotating tool produces local heating and material flow without bulk melting [19]

For similar aluminum sheets, FSW can refine the stirred-zone microstructure and reduce fusion porosity. For dissimilar aluminum-steel blanks, offset and stepped-tool configurations can achieve load transfer and permit subsequent drawing, as demonstrated for 1.0 mm steel joined to 2.0 mm aluminum [21].

Balanced assessment requires the limitations to be stated: hook or kissing-bond defects, incomplete penetration, local precipitate dissolution and softening, surface grooves, exit holes, strong parameter sensitivity, tool wear in hard or dissimilar systems, clamping demands, and lower production rate than high-speed laser welding. These factors can move failure from the base sheet to the stir zone, HAZ, or interface and can invalidate a generic 'stronger weld' assumption [19-22].

PAW and other fusion processes can provide controlled penetration, but the melt-solidification cycle generates an HAZ, residual stress, and microstructural gradients whose severity depends on heat input, travel speed, shielding, sheet grade, and thickness.

Consequently, the same nominal strength or thickness ratio can produce different WLM and failure behavior after LBW, PAW, resistance welding, or FSW. Weld width and process method may appear secondary only when the tested weld remains narrow, defect-free, and mechanically stronger and more ductile than the critical base-sheet region.

Process selection should therefore be made jointly with the forming route and material pair: high-rate fusion welding may be preferable for established steel combinations, whereas FSW may be attractive for selected aluminum or hybrid blanks when interface quality, surface condition, tooling access, and production rate are acceptable.

The review treats welding as one branch of the coupled mechanism framework—not as an isolated preprocessing step and not as a universally subordinate factor.

## 6. FAILURE BEHAVIOR OF TAILOR-WELDED BLANKS

Failure should be classified by both location and triggering mechanism. The two common sketches in Figure 5—fracture at the weld and fracture in the weaker base sheet—are useful but not exhaustive [7, 11].

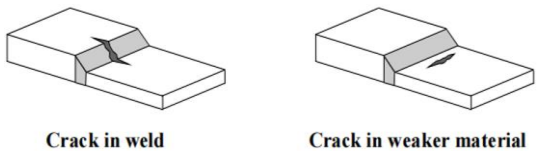



**Figure 5.** Two common, but non-exhaustive, failure locations in tailor-welded blanks (TWBs): fracture at/near the weld and fracture in the weaker base sheet [11]

Weld-metal or stir-zone fracture occurs when a defect, low ductility, underfill, unfavorable interface morphology, or loading parallel to a weak joint makes the joined region critical. Initiation can be governed by joint defects rather than the nominal SR.

HAZ localization is distinct from weld-center fracture. Local softening, hardening-induced strain incompatibility, a narrow ductility trough, or residual stress can concentrate strain beside the weld even when the weld metal itself is stronger than both parent sheets [9, 11].

Weaker-base-sheet necking and fracture occur when the joint transfers load successfully, but mismatch redirects deformation into the lower-strength, thinner, or more ductile sheet. The crack may be parallel to and close to the weld without being a weld fracture [4, 10, 11].

Edge cracking, interface-related separation, and weld-defect initiation must also be reported separately. Under bending/unbending or non-linear strain paths, mixed modes can develop: edge damage may grow into the base sheet, a HAZ neck may link with a weld defect, or interface damage may interact with through-thickness shear.

A complete failure report should therefore state the initiation location, propagation path, local strain path, weld orientation, defect evidence, and whether the criterion predicts necking, ductile damage, shear localization, or interface separation. A single 'weld versus weak sheet' label is insufficient.

## 7. WELD-LINE MOVEMENT DURING DEEP DRAWING

WLM is defined here as the displacement of the formed weld from its initial material coordinate. A positive direction must be specified for each measurement region. For the cup bottom, this review defines positive movement toward the sheet with higher section resistance; wall or flange movement is reported with its observed local direction. This convention is necessary because one cup can show opposite directions at the bottom and wall [2, 10].

The mechanism is a local force and flow imbalance. The more deformable sheet generally draws in and stretches more, while the higher-resistance sheet constrains the interface. Geometry then maps this imbalance differently across the punch bottom, die radius, wall, and flange, so a universal statement that the weld always moves toward either the stronger or weaker sheet is incorrect. The main location-dependent defects associated with WLM are summarized in Figure 6.

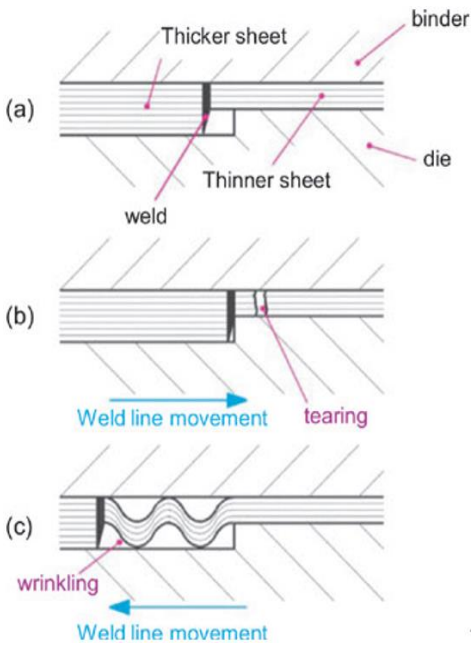



**Figure 6.** Location-dependent defects associated with weld-line movement (WLM) in tailor-welded blanks (TWBs), including non-uniform draw-in, wrinkling, thinning, and tearing during deep drawing

Strength and thickness mismatch are major WLM drivers, but they are not the only controls. Weld/HAZ width and properties, residual stress, anisotropy mismatch, weld orientation, friction, drawbead restraint, blank-holder force, temperature, and defects can change the resistance field and the path by which material enters the die [2, 5, 8, 9, 23].

Weld placement relative to the punch corner and die radius changes both movement and failure risk. Offsetting the weld can allocate more area of the high-resistance sheet to a critical zone and improve LDR, but it can also increase draw-in asymmetry elsewhere; the sign and measurement location must be reported [6, 10, 24].

Control strategies include non-uniform blank holding, adjustable drawbeads, counter pressure, tailored tooling, and local thermal conditioning [5, 6, 14-16]. Their effect is not uniformly 'more restraint equals less WLM': additional restraint can reduce draw-in in one region while increasing local strain, thinning, or movement in another. Optimization must therefore be multi-objective.

WLM is best treated as an evolving state variable linked to local strain and draw-in rather than as a single final displacement. Comparable reporting requires the initial weld geometry, coordinate convention, measurement region, punch stroke, and signed movement.

## 8. SPRINGBACK AND UNLOADING IN TAILOR-WELDED BLANKS

Springback in a TWB is spatially non-uniform because each base sheet and weld-zone subregion reaches a different plastic strain and residual-stress state before unloading. A global homogeneous-sheet calibration cannot reproduce this field when the weld position or material pair changes [25].

The FE model should map the fusion/stir zone and HAZ when their width or property gradients are mechanically significant. Local yield stress, hardening, elastic modulus, thickness, and residual stress determine how bending moments redistribute across the weld during unloading [3, 8, 9, 25].

Residual stress from welding can add to or subtract from forming stress, while local hardening or softening shifts the neutral axis and the plastic-zone depth. The effect is particularly important when the weld crosses a bend radius or when the two sheets have markedly different strength-to-modulus ratios.

Anisotropy mismatch and path-dependent hardening influence both the forming stage and reverse loading. For accurate unloading, constitutive choices should be justified with cyclic or reverse-loading evidence where possible; isotropic hardening alone can underpredict the Bauschinger response and distort springback trends.

A TWB-specific validation should compare local strain and final geometry on both sides of the weld, not only a global opening angle. Digital image correlation, local thickness or hardness mapping, and residual-stress measurements can identify whether error comes from base-sheet calibration, weld-zone mapping, contact, or the unloading law.

For automated compensation, the model should support iterative updating: measured draw-in and WLM during forming can update uncertain friction, restraint, and weld-zone parameters before a die or trajectory correction is applied.

## 9. EVIDENCE SYNTHESIS BY FORMING PROCESS

Table 1 groups the evidence by forming process and reports a common set of technical variables. Deep drawing and stamping dominate the synthesis. Stretch/bulge forming, warm forming, single-point incremental forming, and bending are retained as separate groups because their stress states, strain paths, and formability measures differ. Missing thickness ratios are identified rather than inferred.

**Table 1.** Evidence matrix grouped by forming process and common technical variables

| Study | Common Technical Variables | Direction, Metric, and Failure Result |
|---|---|---|
| Kinsey et al. [1] | Deep drawing \| Material/TR: dissimilar sheets, multiple configurations \| Weld: laser \| Metrics: draw-in and WLM | Mismatch creates asymmetric draw-in; active flow control can reduce WLM. Failure depends on the local constraint field. |
| Choi et al. [2] | Deep drawing \| Material/TR: laser-welded steel, varied blank shape and weld location \| Metrics: WLM and thickness strain | WLM direction and magnitude vary with geometry and measurement location; strain concentrates on the more deformable side. |
| Bandyopadhyay et al. [4] | Deep drawing \| Material: DP600/DP980 steel, equal gauge \| Weld: laser \| Metrics: LDR, strain, fracture | Higher strength mismatch lowers LDR; fracture initiates in the weaker sheet near the weld/HAZ under tested conditions. |
| Asadian-Ardakani et al. [5] | Deep drawing \| Material: IF-steel TWBs, varied thickness ratio \| Weld: laser \| Control: non-uniform BHF \| Metrics: WLM and cup quality | Segmented/non-uniform BHF redistributes draw-in and reduces WLM, but the effective force split is material- and geometry-specific. |
| Mennecart et al. [6] | Deep drawing \| Material: HCT600X/HCT980X tailored blanks \| Weld: laser \| Tool: tailored die/blank holder \| Metrics: cracks, wrinkles, WLM | Tailored tools improve flow balance and delay crack/wrinkle formation; weld placement remains critical. |
| Abdolazimzadeh et al. [23] | Deep drawing \| Material: St37 steel TWBs, varied process parameters \| Weld: fusion \| Metrics: WLM | WLM increases with stronger restraint in the studied setup and decreases with larger tool radii; coordinate convention must be stated. |
| Panzer et al. [21] | Deep drawing \| Material/TR: DX54 steel 1.0 mm/AA6016-T4 2.0 mm \| Weld: FSW \| Metrics: joint failure and drawability | Optimized joint strength exceeded the steel base sheet; thickness-step tooling and interface integrity controlled successful forming. |
| Aminzadeh et al. [24] | Deep drawing \| Material: dissimilar laser-welded sheets \| Weld layout/topology varied \| Metrics: thinning, stress, failure | Optimized weld layout reduced localized stress/thinning; benefit was coupled to material distribution and boundary conditions. |
| Moayedi et al. [12] | Deep drawing/stretching \| Material: thin dissimilar steel sheets \| Weld: laser \| Variable: weld orientation \| Metrics: FLD, strain and failure location | Orientation changes the local strain path and failure location; no orientation is universally optimal across load paths. |
| Hao et al. [9] | Deep drawing \| Material: large steel TWB \| Weld/HAZ: fusion weld with pre-deformation rolling \| Metrics: HAZ thickness and hardness | HAZ pre-deformation reduced property gradients and improved thickness uniformity, showing that weld-process history can be a first-order factor. |
| Kamalvand et al. [22] | Deep drawing \| Material: AA2024-T3/AA7075-T6 \| Weld: FSW; tool shape/speed varied \| Metrics: tensile response, thinning, WLM | Optimized FSW parameters improved formability; poor tool/parameter combinations promoted local thinning and early failure. |
| Kahhal et al. [16] | Deep drawing \| Material: steel TWB \| Control: adjustable drawbead optimized by neural network \| Metrics: WLM and thinning | Data-driven multi-objective control reduced WLM and thinning together, supporting closed-loop forming concepts. |
| Mayavan et al. [10] | Deep drawing \| Material/TR: AISI 304-IS 513 CR2 and CR3, 0.8/0.8 mm \| Weld: CO2 laser, center/offset \| Metrics: SR, FR, LDR, WLM | Cup bottom moved toward stronger AISI 304, while wall/flange movement was toward the weaker sheet; fracture occurred in the weaker soft zone. |
| Phaoniam and Lawanwong [25] | Hat bending/unloading \| Material: advanced high-strength steel TWB; TR not reported in review table \| Weld position varied \| Metric: springback | Weld position changed the through-section stress field and springback, demonstrating the need for spatial property and unloading models. |
| Panda and Kumar [14] | Hydro-mechanical stretch forming \| Material: extra-low-carbon steel TWB; TR varied \| Weld: laser \| Metrics: LDH, WLM, failure | Counter pressure improved strain distribution and formability; results are not directly transferable to deep drawing because the stress path differs. |
| Panda and Kumar [26] | Biaxial stretch forming \| Material: IF/DP600 steel \| Weld: laser \| Metrics: LDH, FR, WLM and failure | Soft-zone behavior and mismatch-controlled localization; stretch-forming sensitivity differed from deep drawing. |
| Leitão et al. [8] | Stretch/formability tests \| Material: aluminium alloy pairs \| Weld: FSW; weld geometry explicitly modeled \| Metrics: strain and failure | Weld geometry and mechanical mismatch materially changed predicted and measured formability; omitting the weld can be non-conservative. |
| Abbasi et al. [27] | Stretch forming \| Material: dissimilar TWBs, varied thickness/strain ratio \| Weld: laser \| Metric: analytical WLM | The force-balance model predicts movement only within its simplified strain-path and constitutive assumptions. |
| Gnibl and Merklein [15] | Warm forming \| Material: high-strength aluminium TWB \| Weld: fusion plus local heat treatment \| Metrics: material flow and thickness | Local thermal conditioning redistributed flow and improved thickness uniformity; thermal history is therefore integral to the mechanism. |
| Parente et al. [20] | Formability testing \| Material: AA5182-H111/AA6016-T4 \| Weld: FSW \| Metrics: FLD/LDH and failure | FSW can retain useful formability, but local weld/HAZ properties and orientation govern fracture. |
| Safdarian [13] | Forming-limit testing \| Material: AISI 304/St12/St14, equal 1 mm \| Weld: CO2 laser \| Metrics: SR, LSR, FLD and LDH | Increasing the difference between SR and LSR reduced the FLD level and LDH; the proposed limit is criterion- and path-dependent. |
| Oleksik et al. [28] | Single-point incremental forming \| Material: steel TWB; TR/material pair reported by study \| Weld: MAG \| Metrics: force, strain, fracture | Incremental forming produced a distinct non-linear strain path; weld/HAZ localization cannot be pooled with deep-drawing evidence. |
| Wu et al. [18] | Limiting-dome-height simulation/validation \| Material: AA5754 aluminium TWBs; TR 1.5:1 and 2:1 with varied thickness differential \| Weld: FSW context \| Metrics: LDH and equivalent strain | Increasing thickness differential changed normalized LDH and local strain even at fixed TR; the selected fracture-strain criterion affected the trend. |

Note: AA, aluminium alloy; BHF, blank-holder force; $CO_2$, carbon dioxide; DP, dual-phase steel; FE, finite element; FLD, forming-limit diagram; FR, formability ratio; FSW, friction stir welding; HAZ, heat-affected zone; IF, interstitial-free steel; LDH, limiting dome height; LDR, limiting drawing ratio; MAG, metal active gas; SR, strength ratio; TR, thickness ratio; TWB, tailor-welded blank; WLM, weld-line movement.

The non-deep-drawing evidence is kept as separate process groups: biaxial stretch-forming studies report distinct forming-limit behavior [26], analytical models address WLM under simplified assumptions [27], and single-point incremental forming introduces a non-linear strain path that is not directly comparable with deep drawing [28].

## 10. AUTOMATION, MONITORING, AND CLOSED-LOOP CONTROL

The mechanism framework creates a direct fit with automated systems: the observable state is not only punch force but also local draw-in, signed WLM, strain localization,

temperature, and final dimensional error. Machine vision or digital image correlation can track the weld and sheet edges; force, displacement, acoustic, and thermal signals can detect instability or weld-zone anomalies.

•A digital process model should combine a spatial weld-zone property map with an FE model and measurement uncertainty. Online WLM and draw-in can be assimilated to update friction, restraint, or local flow parameters rather than waiting for end-of-line failure.

•Adaptive blank-holder segments and adjustable drawbeads provide practical control inputs. Neural-network-assisted optimization has already reduced WLM and thinning in simulation/experiment frameworks, while deep-learning models have optimized non-uniform blank holding for related deep-drawing quality objectives [16, 29].

•The next step is closed-loop multi-objective control: minimize signed WLM and thinning while respecting wrinkle, force, damage, and springback constraints. A controller should be trained and validated across material lots, weld positions, and weld-zone property variation rather than on one nominal simulation.

•Data-driven quality prediction is most credible when features remain mechanically interpretable—strength and thickness mismatch, local hardness or flow stress, weld width, residual stress proxy, draw-in, strain-path measures, force history, and temperature. Industrial ramp-up data can then support surrogate models and constrained optimization, as shown for friction-stir-welded tailored components [30].

Required research priorities are:

•Standardized signed WLM measurements at the bottom, wall/die-radius, and flange regions throughout punch stroke;

•Rapid, spatial weld-zone characterization suitable for FE calibration and in-line quality control;

•Damage and interface models that distinguish weld, HAZ, base-sheet, edge, and mixed failure;

•FE-experiment updating and uncertainty quantification across coils, weld batches, lubrication states, and tool wear; and

•Closed-loop experiments that jointly control WLM, thinning, wrinkling, springback, and cycle time.

## 11. MECHANISTIC SYNTHESIS AND RESEARCH GAPS

Across the evidence, material mismatch defines the initial tendency for asymmetric flow, but the realized response is filtered through weld-zone properties, boundary conditions, and the local strain path. WLM, failure, and springback are therefore linked outcomes of one evolving mechanical system rather than independent defects.

The principal evidence gap is not another isolated correlation. It is a transferable validation framework that reports the resistance map, signed regional WLM, local strain path, failure trigger, and uncertainty using common definitions across welding processes and forming routes.

Process-specific evidence should remain separated until a dimensionless or physics-based mapping demonstrates transfer. In particular, deep drawing, biaxial stretch forming, warm forming, incremental forming, and bending/unloading should not share a single formability ranking without accounting for their different stress paths and metrics.

## 12. CONCLUSIONS

•TWB formability is governed by a coupled resistance field: base-sheet thickness and strength mismatch interact with weld/HAZ properties, residual stress, anisotropy, weld placement, tooling, friction, and restraint.

•No universal WLM direction should be reported without a coordinate convention and measurement location. In a single deep-drawn cup, the bottom may move toward the stronger sheet while the wall or flange moves toward the weaker sheet [10].

•Material mismatch is often a dominant first-order driver, but welding method, weld width and geometry, HAZ gradients, and defects can become first-order controls in soft-zone, hybrid-material, or interface-limited systems.

•Failure must be classified by location and trigger: weld/stir-zone fracture, HAZ localization, weaker-base-sheet necking, edge/interface initiation, and mixed mechanisms under non-linear paths require different models and remedies.

•FR and limit criteria are meaningful only when reference material, thickness, test geometry, loading path, and failure definition are stated. They should not be treated as universal material constants.

•FSW is promising for selected aluminum and hybrid TWBs but is not generally superior to fusion welding; hook defects, local softening, surface condition, tool wear, parameter sensitivity, and cycle rate must be included in the selection decision.

•The most productive research direction for JESA is an automated, closed-loop framework that combines weld-zone mapping, online WLM and strain monitoring, FE-experiment updating, interpretable data-driven quality prediction, and adaptive blank-holder or drawbead control.

## REFERENCES


[1] Kinsey, B., Liu, Z., Cao, J. (2000). A novel forming technology for tailor-welded blanks. Journal of Materials Processing Technology, 99(1-3): 145-153. https://doi.org/10.1016/S0924-0136(99)00412-4

[2] Choi, Y., Heo, Y., Kim, H.Y., Seo, D. (2000). Investigations of weld-line movements for the deep drawing process of tailor welded blanks. Journal of Materials Processing Technology, 108(1): 1-7. https://doi.org/10.1016/S0924-0136(00)00536-7

[3] Raymond, S.D., Wild, P.M., Bayley, C.J. (2004). On modeling of the weld line in finite element analyses of tailor-welded blank forming operations. Journal of Materials Processing Technology, 147(1): 28-37. https://doi.org/10.1016/j.jmatprotec.2003.09.005

[4] Bandyopadhyay, K., Panda, S.K., Saha, P., Padmanabham, G. (2015). Limiting drawing ratio and deep drawing behavior of dual phase steel tailor welded blanks: FE simulation and experimental validation. Journal of Materials Processing Technology, 217: 48-64. https://doi.org/10.1016/j.jmatprotec.2014.10.022

[5] Asadian-Ardakani, M.H., Morovvati, M.R., Mirnia, M.J., Dariani, B.M. (2017). Theoretical and experimental investigation of deep drawing of tailor-welded IF steel blanks with non-uniform blank holder forces. Proceedings of the Institution of Mechanical Engineers, Part B: Journal of Engineering Manufacture, 231(2): 286-300. https://doi.org/10.1177/0954405415577559

[6] Mennecart, T., ul Hassan, H., Güner, A., Ben Khalifa, N., Hosseini, M. (2016). Deep drawing of high-strength tailored blanks by using tailored tools. Materials, 9(2): 77. https://doi.org/10.3390/ma9020077
[7] Bajaj, D., Siddiquee, A.N., Chen, D.L., et al. (2024). Specifics of formability in recent developments of tailor-welded blanks. National Academy Science Letters, 47(4): 451-456. https://doi.org/10.1007/s40009-023-01286-z
[8] Leitão, C., Zhang, B.K., Padmanabhan, R., Rodrigues, D.M. (2011). Influence of weld geometry and mismatch on formability of aluminium tailor welded blanks: Numerical and experimental analysis. Science and Technology of Welding and Joining, 16(8): 662-668. https://doi.org/10.1179/1362171811Y.0000000055
[9] Hao, Z., Luo, J., Jin, Y., Zhang, C. (2020). Application of pre-deformation rolling in the welding heat-affected zone of tailor-welded blanks formed by deep-drawing process. Journal of Manufacturing Processes, 51: 151-160. https://doi.org/10.1016/j.jmapro.2020.01.034
[10] Mayavan, T., Karthikeyan, L., Balamugundan, B., Senthil Kumar, V.S. (2022). Forming of tailor-welded blanks through centerline and offset laser welding. International Journal of Manufacturing, Materials, and Mechanical Engineering, 12(1): 1-14. https://doi.org/10.4018/IJMMME.299059
[11] Bandyopadhyay, K., Lee, M.G., Panda, S.K., Saha, P., Lee, J. (2017). Formability assessment and failure prediction of laser welded dual phase steel blanks using anisotropic plastic properties. International Journal of Mechanical Sciences, 126: 203-221. https://doi.org/10.1016/j.ijmecsci.2017.03.022
[12] Moayedi, H., Darabi, R., Ghabussi, A., Habibi, M., Foong, L.K. (2020). Weld orientation effects on the formability of tailor welded thin steel sheets. Thin-Walled Structures, 149: 106669. https://doi.org/10.1016/j.tws.2020.106669
[13] Safdarian, R. (2018). The effects of strength ratio on the forming limit diagram of tailor-welded blanks. Ironmaking & Steelmaking, 45(1): 17-24. https://doi.org/10.1080/03019233.2016.1235371
[14] Panda, S.K., Kumar, D.R. (2008). Improvement in formability of tailor welded blanks by application of counter pressure in biaxial stretch forming. Journal of Materials Processing Technology, 204(1-3): 70-79. https://doi.org/10.1016/j.jmatprotec.2007.10.076
[15] Gnibl, T., Merklein, M. (2016). Material flow control in tailor welded blanks by a combination of heat treatment and warm forming. CIRP Annals, 65(1): 305-308. https://doi.org/10.1016/j.cirp.2016.04.124
[16] Kahhal, P., Jung, J., Hur, Y.C., Moon, Y.H., Kim, J.H. (2022). Neural network-based multi-objective optimization of adjustable drawbead movement for deep drawing of tailor-welded blanks. Materials, 15(4): 1430. https://doi.org/10.3390/ma15041430
[17] Xing, F., Qiu, X., Lu, Y., Luo, C., Wang, D. (2020). Tailor welded partition blanks: New methods improve the ductility of ultra-high-strength welded joint. ISIJ International, 60(2): 324-329. https://doi.org/10.2355/isijinternational.ISIJINT-2019-114
[18] Wu, J., Hovanski, Y., Miles, M. (2021). Investigation of the thickness differential on the formability of aluminum tailor-welded blanks. Metals, 11(6): 875. https://doi.org/10.3390/met11060875
[19] Mishra, R.S., Ma, Z.Y. (2005). Friction stir welding and processing. Materials Science and Engineering: R: Reports, 50(1-2): 1-78. https://doi.org/10.1016/j.mser.2005.07.001
[20] Parente, M.P.L., Safdarian, R., Santos, A.D., Loureiro, A., Vilaça, P., Jorge, R.M.N. (2016). A study on the formability of aluminum tailor welded blanks produced by friction stir welding. The International Journal of Advanced Manufacturing Technology, 83(9-12): 2129-2141. https://doi.org/10.1007/s00170-015-7950-0
[21] Panzer, F., Schneider, M., Werz, M., Weihe, S. (2019). Friction stir welded and deep drawn multi-material tailor welded blanks. Materials Testing, 61(7): 643-651. https://doi.org/10.3139/120.111366
[22] Kamalvand, E., Jabbari, A., Sheykholeslami, M.R., Mazdak, S., Beygi, R., Mohammadi, S. (2021). Effect of friction stir welding parameters on the deep drawing of tailor-welded blanks. CIRP Journal of Manufacturing Science and Technology, 33: 91-99. https://doi.org/10.1016/j.cirpj.2021.02.011
[23] Abdolazimzadeh, S., Mazdak, S., Sharifi, E., Sheykholeslami, M. (2018). The prediction of weld line movement in deep drawing of tailor welded blanks. Journal of Stress Analysis, 3(1): 1-10. https://doi.org/10.22084/jrstan.2018.15948.1045
[24] Aminzadeh, A., Parvizi, A., Moradi, M. (2020). Multi-objective topology optimization of deep drawing dissimilar tailor laser welded blanks: Experimental and finite element investigation. Optics & Laser Technology, 125: 106029. https://doi.org/10.1016/j.optlastec.2019.106029
[25] Phaoniam, R., Lawanwong, K. (2024). Effect of weld-line position on springback behavior in advanced high-strength steel tailor-welded blanks on hat-shaped bending application. Journal of Advanced Joining Processes, 10: 100241. https://doi.org/10.1016/j.jajp.2024.100241
[26] Panda, S.K., Kumar, D.R. (2010). Experimental and numerical studies on the forming behavior of tailor welded steel sheets in biaxial stretch forming. Materials & Design, 31(3): 1365-1383. https://doi.org/10.1016/j.matdes.2009.08.046
[27] Abbasi, M., Hamzeloo, S.R., Ketabchi, M., Shafaat, M.A., Bagheri, B. (2014). Analytical method for prediction of weld line movement during stretch forming of tailor-welded blanks. The International Journal of Advanced Manufacturing Technology, 73(5-8): 999-1009. https://doi.org/10.1007/s00170-014-5850-3
[28] Oleksik, V., Dobrotă, D., Racz, S.G., Rusu, G.P., Popp, M.O., Avrigean, E. (2021). Experimental research on the behaviour of metal active gas tailor welded blanks during single point incremental forming process. Metals, 11(2): 198. https://doi.org/10.3390/met11020198
[29] Tran, M.T., Shan, Z., Lee, H.W., Kim, D.K. (2021). Earing reduction by varying blank holding force in deep drawing with deep neural network. Metals, 11(3): 395. https://doi.org/10.3390/met11030395
[30] Ackert, P., Idriss, M., Schwarz, C. (2025). Modeling and optimization of a hot forming process for friction stir-welded tailored blanks with an industrially suitable number of test specimens. The International Journal of Advanced Manufacturing Technology, 140(9): 5675-5685. https://doi.org/10.1007/s00170-025-16498-4